Published in final edited form as:
Alcohol. 2015 February ; 49(1): 21–27. doi:10.1016/j.alcohol.2014.07.017.

Withdrawal from chronic intermittent alcohol exposure increases dendritic spine density in the lateral orbitofrontal cortex of mice

Natalie S. McGuier, BS[1], **Audrey E. Padula, BS**[1], **Marcelo F. Lopez, PhD**[2], **John J. Woodward, PhD**[1,2], and **Patrick J. Mulholland, PhD**[1,2,*]

[1]Medical University of South Carolina, Department of Neurosciences, 67 President Street, Charleston, SC 29425

[2]Medical University of South Carolina, Department of Psychiatry & Behavioral Sciences, 67 President Street, Charleston, SC 29425

Abstract

Alcohol use disorders (AUDs) are associated with functional and morphological changes in subfields of the prefrontal cortex. Clinical and preclinical evidence indicates that the orbitofrontal cortex (OFC) is critical for controlling impulsive behaviors, representing the value of a predicted outcome, and reversing learned associations. Individuals with AUDs often demonstrate deficits in OFC-dependent tasks and rodent models of alcohol exposure show that OFC-dependent behaviors are impaired by chronic alcohol exposure. To explore the mechanisms that underlie these impairments, we examined dendritic spine density and morphology, and NMDA-type glutamate receptor expression in the lateral OFC of C57BL/6J mice following chronic intermittent ethanol (CIE) exposure. Western blot analysis demonstrated that NMDA receptors were not altered immediately following CIE exposure or after 7 days of withdrawal. Morphological analysis of basal dendrites of layer II/III pyramidal neurons revealed that dendritic spine density was also not affected immediately after CIE exposure. However, the total density of dendritic spines was significantly increased after a 7 day withdrawal from CIE exposure. The effect of withdrawal on spine density was mediated by an increase in the density of long, thin spines with no change in either stubby or mushroom spines. These data suggest that morphological neuroadaptations in lateral OFC neurons develop during alcohol withdrawal and occur in the absence of changes in the expression of NMDA-type glutamate receptors. The enhanced spine density that follows alcohol withdrawal may contribute to the impairments in OFC-dependent behaviors observed in CIE treated mice.

Keywords

Chronic intermittent ethanol exposure; dendritic spines; lateral OFC; structural plasticity; NMDA receptors

[*]Corresponding Author: Patrick J. Mulholland, PhD, Medical University of South Carolina, Department of Neurosciences, 67 President Street, MSC 861/IOP 462N, Charleston, SC 29425-8610, Phone: 843-792-1229, Fax: 843-792-7353, mulholl@musc.edu.

DISCLOSURE

The authors declare no conflict of interest.

INTRODUCTION

Cognitive and behavioral changes are characteristic symptoms of long-term alcohol (i.e., ethanol) consumption, and include increased anxiety and irritability, memory deficits, and impaired executive function (Abernathy et al., 2010). The prefrontal cortex (PFC) and its subregions regulate executive function, and two of these regions, the medial PFC (mPFC) and the orbitofrontal cortex (OFC), mediate cognitive flexibility and decision-making related to expected rewards, respectively (Fuster, 2008; Zald and Rauch, 2006). The OFC's role in representing the value of a given stimulus is particularly interesting because it not only integrates information from a variety of primary sensory modalities but also participates in abstract concepts such as monetary reward (O'Doherty et al., 2001; O'Doherty, 2004). In addition, evidence suggests that the OFC specifically participates in coding the rewarding aspects rather than the direct sensory aspects of stimuli (O'Doherty et al., 2000). Not surprisingly, this region plays a critical role in regulating impulsive behaviors and reversal learning (Berlin et al., 2004; Schoenbaum et al., 2007; Winstanley et al., 2004). fMRI studies show that patients with alcohol use disorders (AUDs) have greater activation of the OFC when performing OFC-dependent tasks compared to healthy controls, suggesting that prolonged alcohol consumption impairs OFC function, forcing the region to work harder to execute the same task. Outside of the scanner, patients with AUDs also perform poorly on reversal-learning tasks (Fortier et al., 2009; Fortier et al., 2008) in a manner similar to patients with OFC lesions (Hornak et al., 2004; Tsuchida et al., 2010).

Consistent with deficits reported in individuals with AUDs, rodent models of alcohol exposure have been shown to induce OFC-dependent behavioral deficits. For example, a previous study reported that treatment of mice with chronic intermittent ethanol (CIE) exposure in vapor inhalation chambers impaired reversal learning in a naturalistic food foraging task (Badanich et al., 2011) that is sensitive to OFC dysfunction (Bissonette et al., 2008). CIE exposure also altered performance during reversal learning on a choice task in mice that is sensitive to OFC and dorsolateral striatum lesions (DePoy et al., 2013). Forced binge-like alcohol consumption in mice also leads to deficits in reversal learning on the Barnes maze without impairing the initial spatial learning portion of the task (Crews and Boettiger, 2009). Together, the results of these studies suggest that chronic alcohol exposure may disrupt selective regions of the frontal cortex including the OFC. Recently, morphological adaptations in the PFC have been associated with alcohol exposure and subsequent behavioral deficits. In rodents, chronic alcohol exposure and withdrawal leads to changes in dendritic arborization and alterations in dendritic spine density (Holmes et al., 2012; Kim et al., 2014; Kroener et al., 2012). In the OFC, while recent studies have investigated the effects of alcohol on dendritic length (DePoy et al., 2013; Holmes et al., 2012), nothing is known about how CIE exposure affects spine density and morphology in this region.

In the present study we determined the effects of CIE exposure and withdrawal on dendritic spine morphology in the lateral OFC of C57BL/6J mice. We also examined chronic alcohol-induced changes in NMDA receptor expression as studies have linked chronic alcohol exposure with altered NMDA receptors in multiple brain regions including the PFC (Holmes

et al., 2012; Kroener et al., 2012; Lovinger and Roberto, 2013). The results from these studies indicate that neurons in the lateral OFC undergo withdrawal-dependent changes in spine morphology in a manner that is distinct from the medial PFC.

MATERIALS AND METHODS

Animals

Adult male C57BL/6J mice (25 – 30 g; Jackson Laboratories, Bar Harbor, ME) were individually housed under a 12 hr light/dark cycle (lights on at 0200). Rodent chow (Harland Tekland, Madison, WI) and water were available *ad libitum*. Mice were maintained in an AAALAC-accredited facility with automated temperature, humidity, and light cycle control. These studies were approved by the Institutional Animal Care and Use Committee and conducted according to the requirements of the NIH Guide for the Care and Use of Laboratory Animals (2011).

CIE Exposure Procedure

CIE exposure of mice was performed using vapor inhalation chambers as described in previous studies (Becker and Lopez, 2004; Lopez and Becker, 2005). Briefly, mice were exposed to alcohol vapor for 16 hr per day followed by an 8 hr withdrawal in their home cage. This exposure regimen was repeated for 4 consecutive days followed by a 3 day rest period before beginning the next cycle of alcohol vapor exposure. This exposure pattern was repeated for a total of 4 weeks, and control mice were placed in air inhalation chambers following the same parameters. Alcohol levels in the chambers were monitored daily and adjusted as necessary to achieve stable BECs above 175 mg/dl (range: 180.8 – 243.7 mg/dl). BECs in mice were measured weekly by taking a blood sample from the retro-orbital sinus immediately upon removal from the chamber. Prior to each chamber session, mice received intraperitoneal (IP) administration of 1.6 g/kg alcohol in combination with 1 mmol/kg pyrazole (an alcohol dehydrogenase inhibitor) in a final volume of 0.02 ml/g body weight to initiate intoxication. Control mice were similarly handled, but were dosed with pyrazole in saline prior to being placed in air chambers.

Subcellular Fractionation and Western Blot Analysis

Tissue punches were taken from the lateral OFC of control and CIE exposed mice (n = 5–10/group) at 0 and 7 day withdrawal from CIE exposure. Triton X-100 insoluble fractions that are enriched in postsynaptic density proteins were prepared as previously described (Mulholland et al., 2012). Briefly, a Dounce homogenate was prepared and centrifuged at 23,000 × g for 30 min at 4°C. The pellet containing membrane-associated proteins was resuspended with 0.5% Triton X-100 buffer. The suspension was rotated for 15 min at 4°C and then centrifuged at 12,000 × g for 20 min at 4°C, generating detergent soluble and insoluble fractions. The detergent insoluble pellet was solubilized in 2% LDS, and western blots were performed on this fraction following previous methods (Badanich et al., 2013). An aliquot of each sample was taken for determination of protein concentration by the bicinchoninic acid assay (Pierce Biotechnology, Inc., Rockford, IL). The remaining samples were stored at −80°C until immunoblot analysis.

Samples were diluted with NuPAGE 4X LDS sample loading buffer (Invitrogen Corp., Carlsbad, CA; pH 8.5) containing 50 mM dithiothreitol, and samples were denatured for 10 min at 70° C. Five μg of each sample was separated using the Bis-Tris (375 mM resolving buffer and 125 mM stacking buffer, pH 6.4; 7.5% acrylamide) discontinuous buffer system with MOPS electrophoresis buffer (50 mM MOPS, 50 mM Tris, 0.1% SDS, 1 mM EDTA, pH 7.7). Protein was then transferred to Immobilon-P PVDF membranes (Millipore, Bedford, MA) using a semi-dry transfer apparatus (Bio-Rad Laboratories, Hercules, CA). After transfer, blots were washed with phosphate-buffered saline containing 0.1% Tween 20 (PBST) and then blocked with PBST containing 5% nonfat dried milk (NFDM) for 1 hr at room temperature with agitation. The membranes were then incubated overnight at 4°C with primary antibodies diluted in PBST containing 0.5% NFDM and washed in PBST prior to 1 hr incubation at room temperature with horseradish peroxidase conjugated secondary antibodies diluted 1:2000 in PBST. Membranes received a final wash in PBST and the antigen-antibody complex was detected by enhanced chemiluminescence using a ChemiDoc MP Imaging system (Bio-Rad Laboratories, Hercules, CA). The bands were quantified by mean optical density using computer-assisted densitometry with ImageJ v1.41 (National Institutes of Health, USA). Because the use of loading controls (e.g., actin, GAPDH) for normalization in western blot experiments are subject to quantitation errors (Aldridge et al., 2008; Dittmer and Dittmer, 2006), normalization to a total protein stain (i.e., amido black) was used in these studies. Before each study, a series of western blots were performed using different titrations of sample and antibody to establish the linear range for each response. GluN1 antibody was purchased from BD Pharmingen (1:4000; Catalog # 556308; San Jose, CA). GluN1 C2′ antibody was purchased from Chemicon International (1:1000; Catalog # AB5050P; Billerica, MA), GluN2A antibody was purchased from EMD Millipore (1:2000; Catalog # 07-732; Billerica, MA) and GluN2B antibody was purchased from NeuroMab (1:2000; Catalog # 75-097; Davis, CA). Phospho-GluN2B antibody was purchased from Cell Signaling Technology (1:1000; Catalog # 4208; Danvers, MA).

Dendritic Spine Labeling and Morphological Classification

Neuronal labeling and morphological classification of dendritic spines in layer II/III lateral OFC neurons were carried out using previously reported methods (Jung et al., 2011; Kroener et al., 2012). At 0 or 7 day withdrawal from CIE exposure, mice (4–6 mice/group/time point) were anesthetized with urethane (1.2 – 1.5 g/kg, IP) and perfused with 0.1 M phosphate buffer (PB) followed by 1.5% paraformaldehyde (PFA) in PB. Brains were blocked and post-fixed for 30 – 60 min. Next, 150 μm thick coronal slices were prepared using a vibratome. DiI coated tungsten particles (1.3 μm diameter) were delivered to the slices using a modified Helio Gene Gun (Bio-Rad; Hercules, CA) fitted with a polycarbonate filter (3.0 μm pore size; BD Biosciences; San Jose, CA). Slices were left overnight at 4°C in PB to allow the DiI to completely diffuse through labeled neurons and sections were post fixed in 4% PFA for 1 hr at room temperature. After mounting with Prolong Gold Antifade mounting media (Life Technologies; Carlsbad, CA), slices were imaged (3 – 5 dendritic sections/mouse) on a Zeiss Confocal microscope. Images of 2nd order basal dendrites (40 – 60 μm length sections) of layer II/III pyramidal neurons were collected and deconvolved using AutoQuant (Media Cybernetics; Rockville, MD). Imaris XT (Bitplane; Zurich, Switzerland) was used to generate a filament of the dendritic shaft and

spines. Dendritic spines were classified into 4 categories (stubby, long, filopodia, and mushroom) based on the spine length and the width of the spine head and neck, where *L* is spine length, *WH* is spine head width, and *WN* is spine neck width. Long spines were identified as having a $L \geq 0.75$ μm and < 3 μm, mushroom spines had a $L < 3.5$ μm, $WH > 0.35$ μm and a $WH > WN$, stubby spines had a $L < 0.75$ μm, and filopodia were identified as having a $L \geq 3$ μm. Spines were identified using Imaris software by an experimenter that was blind to the experimental groups. Data on dendritic spine parameters were averaged for each dendritic section and were collated from the Imaris output via a custom script written in Python.

Statistical Analyses

Western blot data were analyzed by t-tests comparing the normalized optical density values. Dendritic spine data were analyzed as a mixed model (SAS Proc Mixed) with a first order autoregressive covariance matrix across the sequential slices within mice as previously described (Kroener et al., 2012). All data are reported as mean ± SEM and statistical significance was established with $p < 0.05$.

RESULTS

CIE exposure and withdrawal do not affect NMDA receptor expression in the lateral OFC

Results from previous studies demonstrate that CIE exposure and withdrawal alters NMDA receptor expression in the mPFC (Holmes et al., 2012; Kroener et al., 2012). To determine if a similar neuroadaptation occurs in the lateral OFC, NMDA protein expression was measured in mice that were withdrawn from CIE exposure for 0 or 7 days. As shown in Fig. 1, CIE exposure and withdrawal had no significant effect on the expression of GluN1, GluN2A, or GluN2B subunits of the NMDA receptor in a Triton X-100 insoluble membrane fraction that is enriched in post-synaptic density proteins. As alternative splicing and phosphorylation can affect surface trafficking of NMDA receptors (Goebel et al., 2005; Mu et al., 2003; Okabe et al., 1999; Scott et al., 2001), we also examined different subtypes of the GluN1 subunit and the levels of phosphorylated GluN2B. Levels of GluN1 C2′ and phospho-GluN2B were also not altered by CIE exposure or withdrawal. These findings suggest that, unlike some other regions, CIE exposure and withdrawal does not alter the expression of NMDA-type glutamate receptors in the lateral OFC.

Withdrawal from CIE exposure alters dendritic spine density in the lateral OFC

Morphological adaptations of dendritic spines are associated with learning and memory formation (Bourne and Harris, 2007), and recent studies show that CIE-induced deficits in PFC-dependent behavior are associated with morphological adaptations in the PFC (Holmes et al., 2012; Kroener et al., 2012). Since OFC-dependent behaviors are also impaired in CIE treated mice (Badanich et al., 2011; DePoy et al., 2013), we examined dendritic spine morphology in lateral OFC neurons in air control and CIE exposed mice. As shown in Fig. 2, the thickness of the dendritic segments used for spine analysis were not significantly altered by CIE exposure or withdrawal. Moreover, total spine density on 2nd order branches of basal dendrites from layer II/III pyramidal neurons in the lateral OFC was not altered at the 0 d withdrawal time point [$F(1,4) = 0.22$, $p = 0.66$]. However, spine density was

significantly increased in the basal dendrites of these neurons at the 7 day withdrawal time point [$F(1,7) = 8.59$, $p < 0.05$; Fig. 2D].

Dendritic spines are classified by morphological characteristics (stubby, mushroom, long, or filopodia), and the shape of the spine has been associated with differential expression of glutamate receptors and Ca^{2+}- and cAMP-regulated signaling proteins (Arnsten et al., 2012; Bourne and Harris, 2007; Holtmaat et al., 2006; Paspalas et al., 2013). To determine whether the CIE-induced changes in total spine density were subtype-dependent, we mathematically categorized the spines by morphological type following our previously reported methods (Kroener et al., 2012). As shown in Fig. 3B and 4B, long, thin spines accounted for 66.1 ± 0.02% of total dendritic spines on basal dendrites of layer II/II neurons in alcohol-naïve mice. This is within the range of thin spines reported on pyramidal neurons in cortical Area 46 of rhesus macaques and the PFC of rodents (Bourne and Harris, 2007; Dumitriu et al., 2010; Kroener et al., 2012). Consistent with previous findings in the medial PFC (Kroener et al., 2012; Zuo et al., 2005), filopodia accounted for only 1.3% of the total number of spines and because of their low prevalence, were excluded from further analysis. CIE exposure did not produce significant differences in spine class density, length, volume, terminal point diameter, or mushroom spine head volume at the 0 day withdrawal time point (Fig. 3B–F). In contrast, morphological analysis by spine type at the 7 day withdrawal time point showed a significant increase in the density of long, thin spines [$F(1,7) = 7.20$, $p < 0.05$] (Fig. 4B) with no change in the density of stubby or mushroom spines (Fig. 4C–F). These data indicate that CIE exposure induces selective morphological adaptations of lateral OFC long, thin spines that are withdrawal time dependent.

DISCUSSION

The major finding of the present study is that 7 day withdrawal from CIE exposure increases total spine density in the basal dendrites of layer II/III pyramidal neurons in the lateral OFC. The CIE-induced increase in dendritic spines was mediated by an enhanced prevalence of long, thin spines without changes in mature mushroom-shaped or short stubby spines. Thin spines are enriched in NMDA receptors and Ca^{2+}- and cAMP-regulated signaling proteins, are highly plastic, and are precursors to mushroom “memory” spines (Arnsten et al., 2012; Bourne and Harris, 2007; Holtmaat et al., 2006; Paspalas et al., 2013). Despite the increase in thin spines following CIE exposure and withdrawal, there were no changes in the expression of NMDA receptor subunits, suggesting that the OFC undergoes withdrawal-dependent morphological adaptations in dendritic spines independently of changes in NMDA receptor expression. These data provide the first evidence for adaptations in spine morphology in OFC neurons following chronic alcohol exposure and withdrawal.

Findings from both human postmortem studies and rodent models demonstrate that heavy alcohol consumption or long-term alcohol exposure induces morphological neuroadaptations in dendritic arborization and/or dendritic spines (Carpenter-Hyland and Chandler, 2007; Cui et al., 2013; Mulholland and Chandler, 2007). For example, postmortem studies in alcoholics showed that heavy drinking was associated with reductions in apical spine density in layer V pyramidal neurons in Brodmann area (BA) 6 (premotor cortex and supplemental motor area) (Ferrer et al., 1986) and retraction of the dendritic arbor of layer III basal

dendrites in BA4 (motor cortex) and BA8 (superior frontal gyrus) (Harper and Corbett, 1990). Two recent studies have examined the effects of chronic ethanol exposure on the length of basal and apical dendrites of lateral OFC and medial PFC neurons 3 days after withdrawal (Holmes et al., 2012; DePoy et al 2013). They reported that a 3 day withdrawal from CIE exposure induced hypertrophy of distal apical non-terminal dendrites and dendritic retraction of proximal apical dendrites of prelimbic (PL) medial PFC pyramidal neurons but did not affect arborization of pyramidal neurons in the OFC or infralimbic (IL) medial PFC. As these studies did not measure spine density or sub-type, it is unknown whether these parameters were also affected at the 3 day withdrawal time point. In the present study, changes in spine density and sub-type were only observed at the 7 day withdrawal time point, suggesting that changes in dendritic morphology are highly time-dependent and that changes in spine density can occur in the absence of alterations in spine length. This conclusion is supported by findings from previous reports showing that dendrite and spine reorganization can occur independently (Drakew et al., 1999; Kolb et al., 2008). We previously reported that while total spine density on basal dendrites of layer V PL medial PFC neurons was not altered at 0 and 7 days withdrawal from CIE exposure, the density of mature mushroom-shaped spines was increased (Kroener et al., 2012). A more recent study using Wistar rats demonstrated that 3 hr withdrawal from CIE exposure produced retraction of distal apical dendrites and hypertrophy of basal and proximal apical dendrites of layer II/III PL and IL medial PFC neurons (Kim et al., 2014). Similar to our findings in the lateral OFC, this study showed that CIE exposure also increased overall spine density in layer II/III medial PFC neurons without altering the density of mushroom-shaped spines (Kim et al., 2014). Together, these findings illustrate that alcohol-associated changes in dendrite and dendritic spine morphology in the PFC are complex and depend on sub-region, cortical layer, and time since withdrawal.

As discussed above, several studies showed that alcohol induced impairments in behavior were associated with selective morphological adaptations in neuronal arborization and dendritic spine density of PFC neurons (Holmes et al., 2012; Kroener et al., 2012). In a previous study, CIE exposure of C57BL/6J mice produced impaired performance on an OFC-dependent reversal learning task when measured 3 but not 10 days following withdrawal (Badanich et al., 2011). Although that study did not examine spine density of morphology, results from the present study show that CIE exposure increases total and long spine density of basal dendrites of layer II/III pyramidal neurons in the lateral OFC at the 7 day withdrawal period. While it is not yet clear how a CIE-induced increase in long spines may influence behavior, basal dendrites on neurons in superficial layers I and II/III of the neocortex generally receive afferents from long-range inputs, and their efferents generate ipsilateral and contralateral corticocortical connections (Douglas and Martin, 2004; Little and Carter, 2012). A recent study has demonstrated that inputs onto layer II PL medial PFC neurons target specific subpopulations of dendritic spines in a region-selective manner (Little and Carter, 2012). For example, long-range inputs from the midline thalamus selectively form synapses on spines with larger head volumes, while afferents from basolateral amygdala (BLA) and ventral hippocampus target intermediate-sized spines, and contralateral medial PFC inputs innervate spines with smaller head volumes (Little and Carter, 2012). Many regions including the BLA send dense glutamatergic projections to the

OFC (Carmichael and Price, 1995; Ghashghaei and Barbas, 2002; Ray and Price, 1992; Wassum et al., 2012), and while speculative, it is possible that the increase in long spine density of layer II/III neurons observed in the present study reflects a strengthening of the connections between the lateral OFC and subcortical structures during withdrawal from CIE exposure. Although outputs to subcortical structures are thought to arise primarily from deep layer pyramidal neurons, a recent study using a monosynaptic rabies tracing protocol showed that a significant portion of layer II/III pyramidal neurons in the OFC send afferents to subcortical structures (Wall et al., 2013). Thus, CIE-induced adaptations in basal dendritic spines may reflect aberrant connectivity and processing within the cortex and to subcortical structures and may contribute to impaired function of the OFC. Alternatively, recent evidence suggests that pharmacological treatments that prevent age-related cognitive impairments increase the density of long, thin spines on layer III pyramidal neurons in the PFC (Hao et al., 2006). This suggests that the increase in thin spines observed in the present study may result from a homeostatic adaptation that serves to restore the potential for learning-related plasticity in the OFC. Although largely correlative, this contention is supported by evidence showing that the deficit on the reversal learning task in the CIE exposed mice was no longer present at the 10 day withdrawal time point (Badanich et al., 2011).

In the present study, CIE exposure did not induce significant changes in the expression of NMDA receptor subunits either immediately after CIE exposure or following the 7 day withdrawal period. This finding was initially surprising given the body of evidence that chronic alcohol exposure alters NMDA receptor protein and gene expression in various brain areas (Lovinger and Roberto, 2013). However, in many of those regions, NMDA-mediated responses are significantly inhibited by alcohol concentrations achieved during CIE exposure (~200 mg/dL; 44 mM) while NMDA receptors in lateral OFC neurons are only modestly inhibited by even higher concentrations (Badanich et al., 2013). In addition, within the mPFC, there is conflicting evidence on what effects chronic alcohol exposure has on NMDA receptor subunit expression and function. Holmes et al. (2012) reported that GluN1 expression in a crude tissue fraction was decreased 3 days after CIE exposure whereas Kroener et al. (2012) found increased GluN1 and GluN2B expression in PSD-enriched samples from mice examined immediately after CIE treatment and no change in those that underwent a 7 day withdrawal. These studies also reported opposite changes in NMDA receptor function with Holmes et al. showing reduced amplitude of NMDA EPSCs in mPFC neurons 3 days after CIE treatment and Kroener et al. reporting increased NMDA currents at day 0 with less effect at 7 days withdrawal. While these apparent discrepancies may be due to specific methodological differences between these studies, they also suggest that glutamatergic neurotransmission in frontal cortical regions may undergo dynamic changes following alcohol exposure that are driven by powerful homeostatic mechanisms that govern neuronal excitability. As these processes attempt to restore normal signaling in prefrontal regions, they may experience a significant under- and overshoot of the pre-alcohol set point that are captured by measures made at discrete time periods during withdrawal. This oscillation is consistent with some models of drug addiction where repeated cycles of intoxication and withdrawal are proposed to drive allostatic adaptations in neuronal

signaling molecules that result in an altered balance of excitatory and inhibitory neurotransmission (Koob, 2003, 2004, 2013).

In summary, the results from this study show that there are significant and selective adaptations in spine density of basal dendrites in pyramidal neurons in the lateral OFC that are apparent 7 days after withdrawal from chronic alcohol exposure. This observation coupled with those previously reported in the literature suggest that changes in executive function in individuals with alcohol use disorders may result from alterations in structural and functional characteristics of neurons in orbitofrontal and prefrontal regions of the cortex.

Acknowledgments

FUNDING

This work was supported by a pilot project funded by the Charleston Alcohol Research Center (P50 AA010761) and NIH grants AA020930 (PJM) and AA010761 (JJW). NSM is supported by NIH grant AA021618.

The authors would like to sincerely thank Jason Emory Parker and Julia Moss for their technical assistance in the completion of some aspects of these studies. The authors would also like to thank Andrew McGuier for writing the Python script to collate the dendritic spine data exported from the ImarisXT imaging program.

References

Abernathy K, Chandler LJ, Woodward JJ. Alcohol and the prefrontal cortex. International review of neurobiology. 2010; 91:289–320. [PubMed: 20813246]

Aldridge GM, Podrebarac DM, Greenough WT, Weiler IJ. The use of total protein stains as loading controls: an alternative to high-abundance single-protein controls in semi-quantitative immunoblotting. Journal of neuroscience methods. 2008; 172:250–254. [PubMed: 18571732]

Arnsten AF, Wang MJ, Paspalas CD. Neuromodulation of thought: flexibilities and vulnerabilities in prefrontal cortical network synapses. Neuron. 2012; 76:223–239. [PubMed: 23040817]

Badanich KA, Becker HC, Woodward JJ. Effects of chronic intermittent ethanol exposure on orbitofrontal and medial prefrontal cortex-dependent behaviors in mice. Behavioral neuroscience. 2011; 125:879–891. [PubMed: 22122149]

Badanich KA, Mulholland PJ, Beckley JT, Trantham-Davidson H, Woodward JJ. Ethanol reduces neuronal excitability of lateral orbitofrontal cortex neurons via a glycine receptor dependent mechanism. Neuropsychopharmacology: official publication of the American College of Neuropsychopharmacology. 2013; 38:1176–1188. [PubMed: 23314219]

Becker HC, Lopez MF. Increased Ethanol Drinking After Repeated Chronic Ethanol Exposure and Withdrawal Experience in C57BL/6 Mice. Alcoholism: Clinical & Experimental Research. 2004; 28:1829–1838.

Berlin HA, Rolls ET, Kischka U. Impulsivity, time perception, emotion and reinforcement sensitivity in patients with orbitofrontal cortex lesions. Brain: a journal of neurology. 2004; 127:1108–1126. [PubMed: 14985269]

Bissonette GB, Martins GJ, Franz TM, Harper ES, Schoenbaum G, Powell EM. Double dissociation of the effects of medial and orbital prefrontal cortical lesions on attentional and affective shifts in mice. The Journal of neuroscience: the official journal of the Society for Neuroscience. 2008; 28:11124–11130. [PubMed: 18971455]

Bourne J, Harris KM. Do thin spines learn to be mushroom spines that remember? Current opinion in neurobiology. 2007; 17:381–386. [PubMed: 17498943]

Carmichael ST, Price JL. Limbic connections of the orbital and medial prefrontal cortex in macaque monkeys. The Journal of comparative neurology. 1995; 363:615–641. [PubMed: 8847421]

Carpenter-Hyland EP, Chandler LJ. Adaptive plasticity of NMDA receptors and dendritic spines: implications for enhanced vulnerability of the adolescent brain to alcohol addiction. Pharmacology, biochemistry, and behavior. 2007; 86:200–208.

Crews FT, Boettiger CA. Impulsivity, frontal lobes and risk for addiction. Pharmacology, biochemistry, and behavior. 2009; 93:237–247.

Cui C, Noronha A, Morikawa H, Alvarez VA, Stuber GD, Szumlinski KK, Kash TL, Roberto M, Wilcox MV. New insights on neurobiological mechanisms underlying alcohol addiction. Neuropharmacology. 2013; 67:223–232. [PubMed: 23159531]

DePoy L, Daut R, Brigman JL, MacPherson K, Crowley N, Gunduz-Cinar O, Pickens CL, Cinar R, Saksida LM, Kunos G, et al. Chronic alcohol produces neuroadaptations to prime dorsal striatal learning. Proceedings of the National Academy of Sciences of the United States of America. 2013; 110:14783–14788. [PubMed: 23959891]

Dittmer A, Dittmer J. Beta-actin is not a reliable loading control in Western blot analysis. Electrophoresis. 2006; 27:2844–2845. [PubMed: 16688701]

Douglas RJ, Martin KA. Neuronal circuits of the neocortex. Annual review of neuroscience. 2004; 27:419–451.

Drakew A, Frotscher M, Heimrich B. Blockade of neuronal activity alters spine maturation of dentate granule cells but not their dendritic arborization. Neuroscience. 1999; 94:767–774. [PubMed: 10579567]

Dumitriu D, Hao J, Hara Y, Kaufmann J, Janssen WG, Lou W, Rapp PR, Morrison JH. Selective changes in thin spine density and morphology in monkey prefrontal cortex correlate with aging-related cognitive impairment. The Journal of neuroscience: the official journal of the Society for Neuroscience. 2010; 30:7507–7515. [PubMed: 20519525]

Ferrer I, Fabregues I, Rairiz J, Galofre E. Decreased numbers of dendritic spines on cortical pyramidal neurons in human chronic alcoholism. Neuroscience letters. 1986; 69:115–119. [PubMed: 3748463]

Fortier CB, Maksimovskiy AL, Venne JR, LaFleche G, McGlinchey RE. Silent trace eliminates differential eyeblink learning in abstinent alcoholics. International journal of environmental research and public health. 2009; 6:2007–2027. [PubMed: 19742168]

Fortier CB, Steffen EM, Lafleche G, Venne JR, Disterhoft JF, McGlinchey RE. Delay discrimination and reversal eyeblink classical conditioning in abstinent chronic alcoholics. Neuropsychology. 2008; 22:196–208. [PubMed: 18331162]

Fuster, JM. The Prefrontal Cortex. 4. China: Elsevier; 2008.

Ghashghaei HT, Barbas H. Pathways for emotion: interactions of prefrontal and anterior temporal pathways in the amygdala of the rhesus monkey. Neuroscience. 2002; 115:1261–1279. [PubMed: 12453496]

Goebel SM, Alvestad RM, Coultrap SJ, Browning MD. Tyrosine phosphorylation of the N-methyl-D-aspartate receptor is enhanced in synaptic membrane fractions of the adult rat hippocampus. Brain research Molecular brain research. 2005; 142:65–79. [PubMed: 16257472]

Hao J, Rapp PR, Leffler AE, Leffler SR, Janssen WG, Lou W, McKay H, Roberts JA, Wearne SL, Hof PR, et al. Estrogen alters spine number and morphology in prefrontal cortex of aged female rhesus monkeys. The Journal of neuroscience: the official journal of the Society for Neuroscience. 2006; 26:2571–2578. [PubMed: 16510735]

Harper C, Corbett D. Changes in the basal dendrites of cortical pyramidal cells from alcoholic patients--a quantitative Golgi study. Journal of neurology, neurosurgery, and psychiatry. 1990; 53:856–861.

Holmes A, Fitzgerald PJ, MacPherson KP, DeBrouse L, Colacicco G, Flynn SM, Masneuf S, Pleil KE, Li C, Marcinkiewcz CA, et al. Chronic alcohol remodels prefrontal neurons and disrupts NMDAR-mediated fear extinction encoding. Nature neuroscience. 2012; 15:1359–1361.

Holtmaat A, Wilbrecht L, Knott GW, Welker E, Svoboda K. Experience-dependent and cell-type-specific spine growth in the neocortex. Nature. 2006; 441:979–983. [PubMed: 16791195]

Hornak J, O'Doherty J, Bramham J, Rolls ET, Morris RG, Bullock PR, Polkey CE. Reward-related reversal learning after surgical excisions in orbito-frontal or dorsolateral prefrontal cortex in humans. Journal of cognitive neuroscience. 2004; 16:463–478. [PubMed: 15072681]

Jung CK, Fuhrmann M, Honarnejad K, Van Leuven F, Herms J. Role of presenilin 1 in structural plasticity of cortical dendritic spines in vivo. Journal of neurochemistry. 2011; 119:1064–1073. [PubMed: 21951279]

Kim A, Zamora-Martinez ER, Edwards S, Mandyam CD. Structural reorganization of pyramidal neurons in the medial prefrontal cortex of alcohol dependent rats is associated with altered glial plasticity. Brain structure & function. 2014

Kolb B, Cioe J, Comeau W. Contrasting effects of motor and visual spatial learning tasks on dendritic arborization and spine density in rats. Neurobiology of learning and memory. 2008; 90:295–300. [PubMed: 18547826]

Koob GF. Alcoholism: allostasis and beyond. Alcoholism, clinical and experimental research. 2003; 27:232–243.

Koob GF. A role for GABA mechanisms in the motivational effects of alcohol. Biochemical pharmacology. 2004; 68:1515–1525. [PubMed: 15451394]

Koob GF. Theoretical frameworks and mechanistic aspects of alcohol addiction: alcohol addiction as a reward deficit disorder. Current topics in behavioral neurosciences. 2013; 13:3–30. [PubMed: 21744309]

Kroener S, Mulholland PJ, New NN, Gass JT, Becker HC, Chandler LJ. Chronic alcohol exposure alters behavioral and synaptic plasticity of the rodent prefrontal cortex. PloS one. 2012; 7:e37541. [PubMed: 22666364]

Little JP, Carter AG. Subcellular synaptic connectivity of layer 2 pyramidal neurons in the medial prefrontal cortex. The Journal of neuroscience: the official journal of the Society for Neuroscience. 2012; 32:12808–12819. [PubMed: 22973004]

Lopez MF, Becker HC. Effect of pattern and number of chronic ethanol exposures on subsequent voluntary ethanol intake in C57BL/6J mice. Psychopharmacology. 2005; 181:688–696. [PubMed: 16001125]

Lovinger DM, Roberto M. Synaptic effects induced by alcohol. Current topics in behavioral neurosciences. 2013; 13:31–86. [PubMed: 21786203]

Mu Y, Otsuka T, Horton AC, Scott DB, Ehlers MD. Activity-dependent mRNA splicing controls ER export and synaptic delivery of NMDA receptors. Neuron. 2003; 40:581–594. [PubMed: 14642281]

Mulholland PJ, Chandler LJ. The thorny side of addiction: adaptive plasticity and dendritic spines. The Scientific World Journal. 2007; 7:9–21.

Mulholland PJ, Jordan BA, Chandler LJ. Chronic ethanol up-regulates the synaptic expression of the nuclear translational regulatory protein AIDA-1 in primary hippocampal neurons. Alcohol. 2012; 46:569–576. [PubMed: 22703994]

O'Doherty J, Kringelbach ML, Rolls ET, Hornak J, Andrews C. Abstract reward and punishment representations in the human orbitofrontal cortex. Nature neuroscience. 2001; 4:95–102.

O'Doherty J, Rolls ET, Francis S, Bowtell R, McGlone F, Kobal G, Renner B, Ahne G. Sensory-specific satiety-related olfactory activation of the human orbitofrontal cortex. Neuroreport. 2000; 11:399–403. [PubMed: 10674494]

O'Doherty JP. Reward representations and reward-related learning in the human brain: insights from neuroimaging. Current opinion in neurobiology. 2004; 14:769–776. [PubMed: 15582382]

Okabe S, Miwa A, Okado H. Alternative splicing of the C-terminal domain regulates cell surface expression of the NMDA receptor NR1 subunit. The Journal of neuroscience: the official journal of the Society for Neuroscience. 1999; 19:7781–7792. [PubMed: 10479681]

Paspalas CD, Wang M, Arnsten AF. Constellation of HCN channels and cAMP regulating proteins in dendritic spines of the primate prefrontal cortex: potential substrate for working memory deficits in schizophrenia. Cerebral cortex. 2013; 23:1643–1654. [PubMed: 22693343]

Ray JP, Price JL. The organization of the thalamocortical connections of the mediodorsal thalamic nucleus in the rat, related to the ventral forebrain-prefrontal cortex topography. The Journal of comparative neurology. 1992; 323:167–197. [PubMed: 1401255]

Schoenbaum G, Saddoris MP, Stalnaker TA. Reconciling the roles of orbitofrontal cortex in reversal learning and the encoding of outcome expectancies. Annals of the New York Academy of Sciences. 2007; 1121:320–335. [PubMed: 17698988]

Scott DB, Blanpied TA, Swanson GT, Zhang C, Ehlers MD. An NMDA receptor ER retention signal regulated by phosphorylation and alternative splicing. The Journal of neuroscience: the official journal of the Society for Neuroscience. 2001; 21:3063–3072. [PubMed: 11312291]

Tsuchida A, Doll BB, Fellows LK. Beyond reversal: a critical role for human orbitofrontal cortex in flexible learning from probabilistic feedback. The Journal of neuroscience: the official journal of the Society for Neuroscience. 2010; 30:16868–16875. [PubMed: 21159958]

Wall NR, De La Parra M, Callaway EM, Kreitzer AC. Differential innervation of direct- and indirect-pathway striatal projection neurons. Neuron. 2013; 79:347–360. [PubMed: 23810541]

Wassum KM, Tolosa VM, Tseng TC, Balleine BW, Monbouquette HG, Maidment NT. Transient extracellular glutamate events in the basolateral amygdala track reward-seeking actions. The Journal of neuroscience: the official journal of the Society for Neuroscience. 2012; 32:2734–2746. [PubMed: 22357857]

Winstanley CA, Theobald DE, Cardinal RN, Robbins TW. Contrasting roles of basolateral amygdala and orbitofrontal cortex in impulsive choice. The Journal of neuroscience: the official journal of the Society for Neuroscience. 2004; 24:4718–4722. [PubMed: 15152031]

Zald, DH.; Rauch, SL. The Orbitofrontal Cortex. Oxford: Oxford University Press; 2006.

Zuo Y, Lin A, Chang P, Gan WB. Development of long-term dendritic spine stability in diverse regions of cerebral cortex. Neuron. 2005; 46:181–189. [PubMed: 15848798]

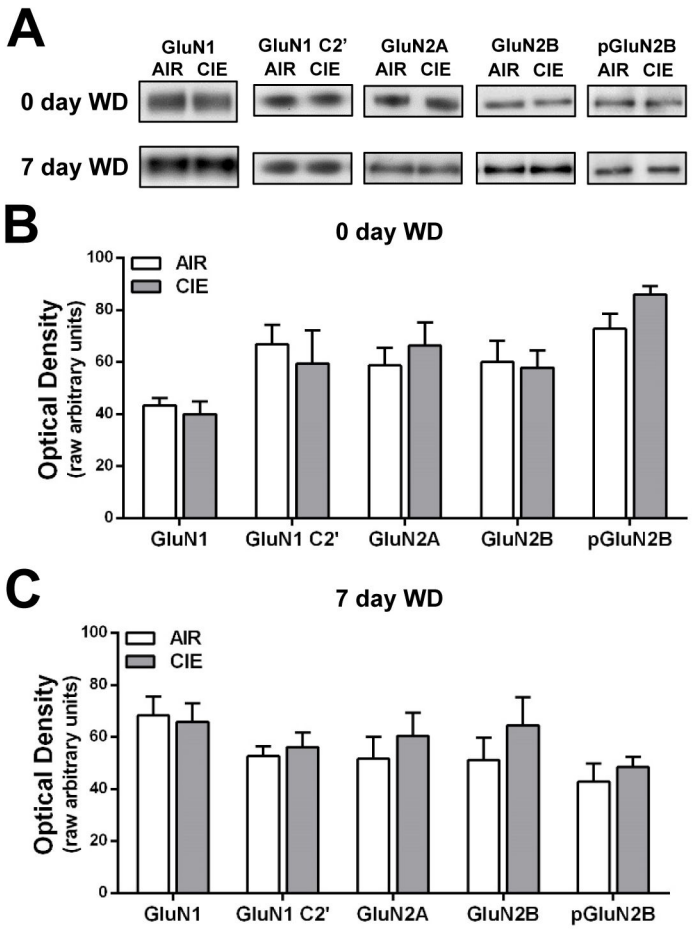

Figure 1.

CIE exposure and withdrawal does not alter NMDA-type glutamate receptor subunit expression in the lateral OFC. **(A)** Representative western blots of NMDA-type glutamate receptor subunits in that lateral OFC of mice withdrawn from CIE exposure for 0 or 7 days. **(B, C)** NMDA receptor subunit expression was not altered as a result of CIE exposure at 0 or 7 days withdrawal ($p > 0.05$ for all two-tailed t-tests; n = 5–10 mice/group).

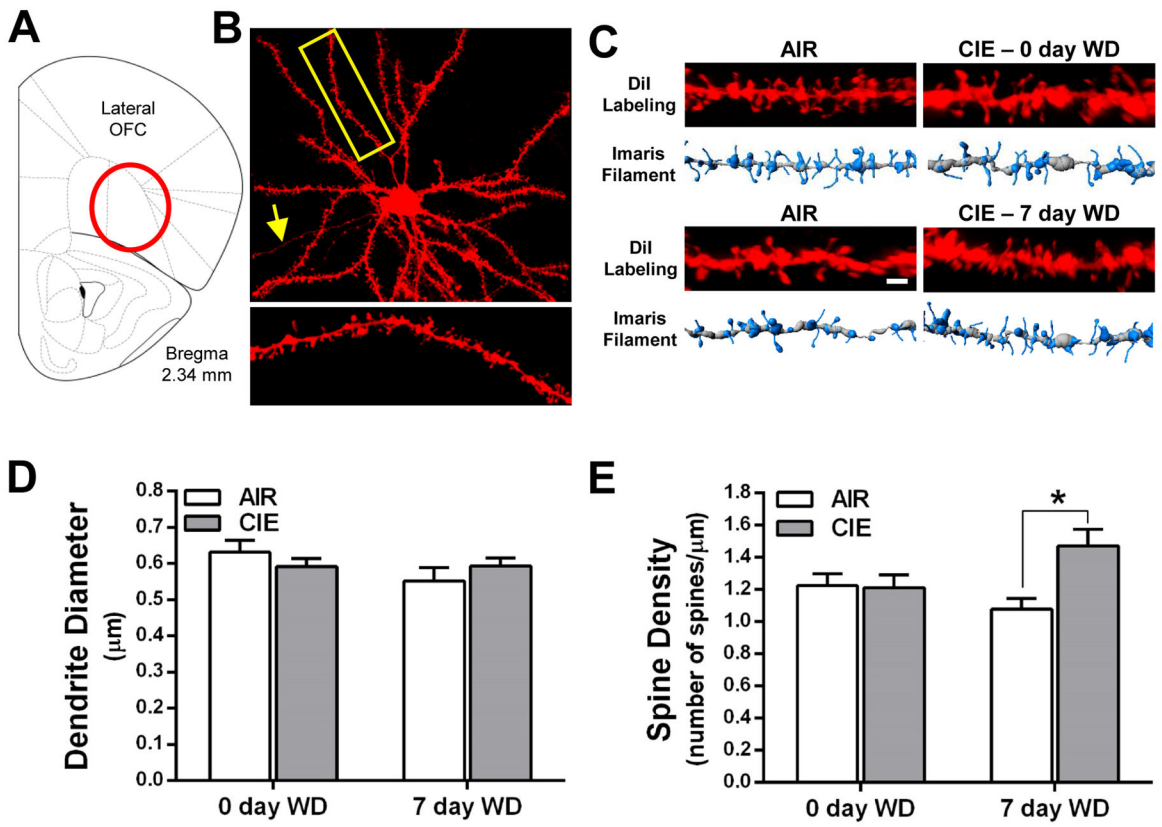

Figure 2.

Withdrawal from CIE exposure increases total spine density of layer II/III neurons in the lateral OFC. **(A)** Schematic depicting the OFC with the lateral OFC highlighted as the target brain region. **(B)** An example of a lateral OFC layer II/III pyramidal neuron filled with DiI. The yellow box and associated enlarged image provide an example of a second order dendritic segment and its dendritic spines. **(C)** Representative images and 3D models generated in Imaris XT at the 0 day (top panel) and 7 day (bottom panel) withdrawal time points. **(D)** CIE exposure and withdrawal did not alter the diameter of basal dendrites of layer II/III pyramidal neurons [two-way ANOVA: $F(1,29) = 0.0012$, $p = 0.973$). **(E)** Total spine density is increased in CIE mice at 7 days withdrawal but not at 0 day withdrawal [0 day WD: $F(1,4) = 0.22$, $p = 0.66$; 7 day WD: $F(1,7) = 8.59$, $^*p < 0.05$].

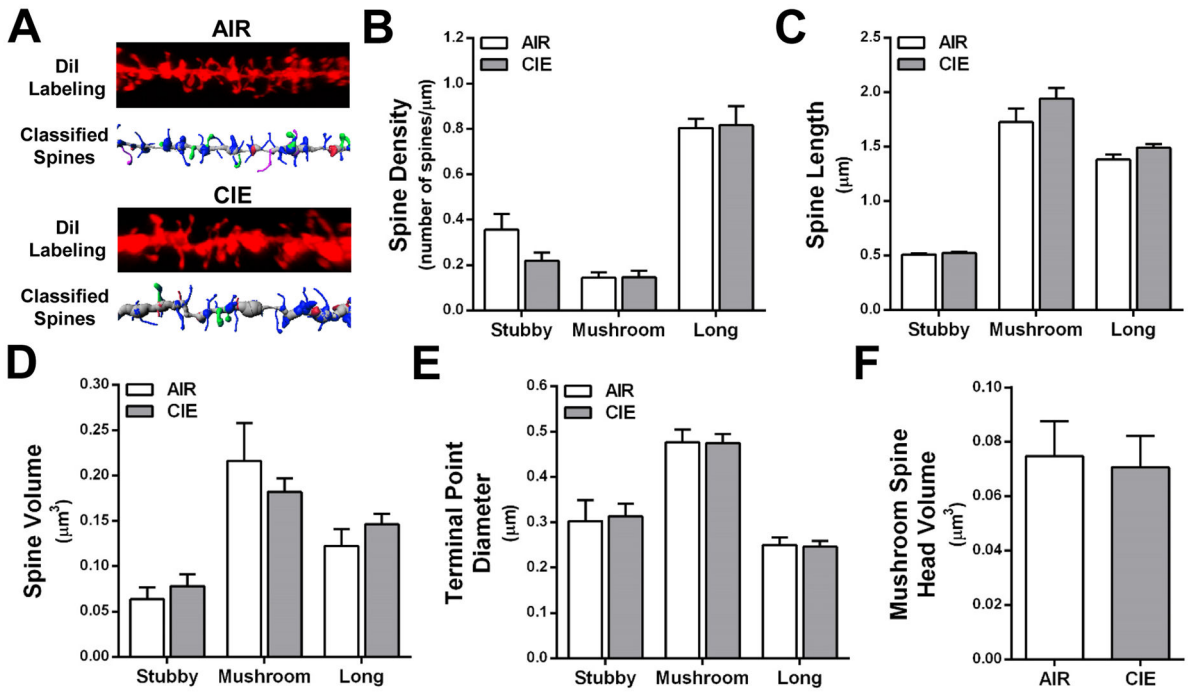

Figure 3.

CIE exposure in the absence of withdrawal does not alter dendritic spines of layer II/III neurons in the lateral OFC. **(A)** Representative images of control (top) and CIE (bottom) dendrite segments and filament from Figure 2C showing classified spines. **(B–E)** When analyzed by spine type (stubby, mushroom, and long), CIE and 0 day withdrawal did not affect spine density, length, volume, or terminal point diameter ($p > 0.05$ for all analyses). **(F)** Head volume of mushroom spines was also unaffected by CIE exposure.

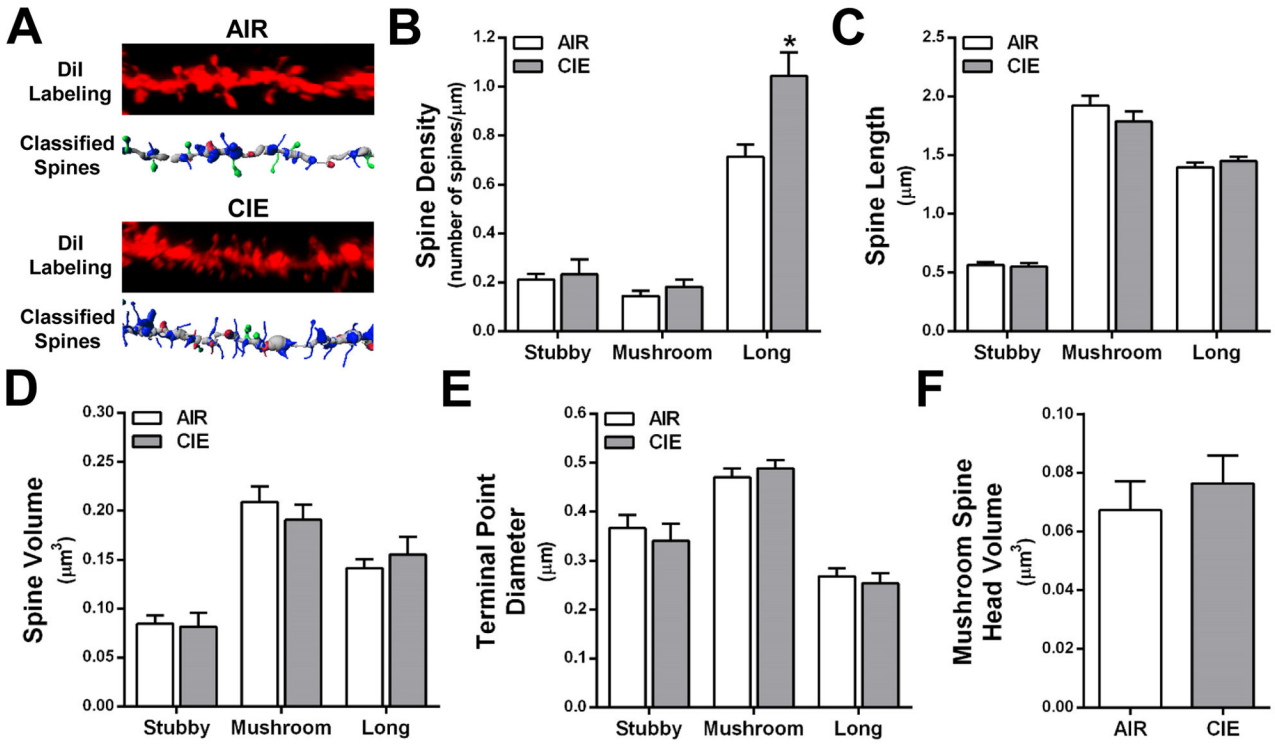

Figure 4.

CIE exposure and 7 day withdrawal increases long, thin spines on basal dendrites of layer II/III neurons in the lateral OFC. **(A)** Representative images of control (top) and CIE (bottom) dendrite segments and filament from Figure 2C showing classified spines. **(B)** Long spine density was significantly increased as a result of CIE exposure and 7 day withdrawal [$F(1,7) = 7.20$, $^*p < 0.05$]. **(C–F)** There was no effect of CIE exposure and 7 day withdrawal on spine length, volume, terminal point diameter or mushroom head volume ($p > 0.05$ for all analyses).